Major drivers of soil acidification over 30 years differ in paddy and upland soils in China

Science of the Total Environment

Xu, Donghao; Ros, Gerard H.; Zhu, Qichao; Xu, Minggang; Wen, Shilin et al

https://doi.org/10.1016/j.scitotenv.2024.170189

Science of the Total Environment 916 (2024) 170189

Contents lists available at ScienceDirect

Science of the Total Environment

journal homepage: www.elsevier.com/locate/scitotenv

Major drivers of soil acidification over 30 years differ in paddy and upland soils in China

Donghao Xu [a,b], Gerard H. Ros [a], Qichao Zhu [b,*], Minggang Xu [c], Shilin Wen [d], Zejiang Cai [d], Fusuo Zhang [b], Wim de Vries [a]

[a] Wageningen University and Research, Environmental Systems Analysis Group, PO Box 47, 6700AA Wageningen, the Netherlands
[b] College of Resources and Environmental Sciences, National Academy of Agriculture Green Development, China Agricultural University, 100193 Beijing, China
[c] Institute of Agricultural Resources and Regional Planning, Chinese Academy of Agricultural Sciences, Beijing 100081, China
[d] Hengyang Red Soil Experimental Station, Chinese Academy of Agricultural Science, Hengyang 421001, China

HIGHLIGHTS

- The VSD+ model well reconstructed soil acidification history at county level.
- Bicarbonate leaching was an important driver of acidity production in paddy soils.
- Nitrogen transformations mainly drove acidity production in upland soils.
- Reducing bicarbonate leaching is key to mitigate soil acidification in paddy soils.
- Balancing nitrogen input is key to mitigate soil acidification in upland soils.

GRAPHICAL ABSTRACT

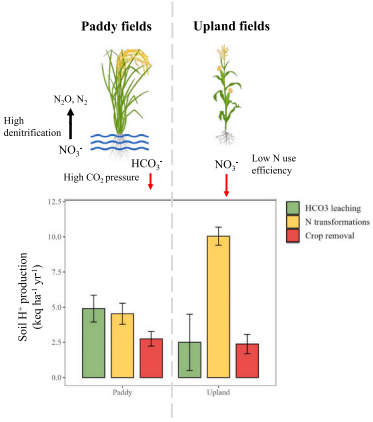

ARTICLE INFO

Editor: Jay Gan

Keywords:
VSD+ model
Paddy
Upland
Soil acidification
Agricultural management

ABSTRACT

Elevated nitrogen (N) fertilization has largely increased crop production in China, but also increased acidification risks, thereby threatening crop yields. However, natural soil acidification due to bicarbonate (HCO_3) leaching and base cation (BC) removal by crop harvest also affect soil acidity whereas the input of HCO_3 and BC via fertilizers and manure counteract soil acidification. Insights in rates and drivers of soil acidification in different land use types is too limited to support crop- and site-specific mitigation strategies. In this study, we assessed the historical changes in cropland acidification rates and their drivers for the period 1985–2019 at 151 sites in a typical Chinese county with the combined nutrient and soil acidification model VSD+. VSD+ could well reproduce long-term changes in pH and in the BC concentrations of calcium, magnesium and potassium between 1985 and 2019 in non-calcareous soils. In paddy soils, the acidity production rate decreased from 1985 onwards, mainly driven by a pH-induced reduction in HCO_3 leaching and N transformations. In upland soils, however, acidity production was mainly driven by N transformations and hardly changed over time. Crop BC removal by

* Corresponding author.
E-mail address: qichaozhu@126.com (Q. Zhu).

https://doi.org/10.1016/j.scitotenv.2024.170189
Received 18 November 2023; Received in revised form 9 January 2024; Accepted 13 January 2024
Available online 19 January 2024

harvesting played a minor role in both paddy and upland soils, but its relative importance increased in paddy soils. The acidity input was partly neutralized by HCO_3 input from fertilizers and manure, which decreased over time due to a change from ammonia bicarbonate to urea. Soil buffering by both BC and aluminium release decreased in paddy soils due to a reduction in net acidity production, while it stayed relatively constant in upland soils. We conclude that acidification management in paddy soils requires a focus on avoiding high HCO_3 leaching whereas the management in upland soils should focus on balancing N with recycling organic manure and crop residues.

1. Introduction

Healthy soils are critical for global food production and human well-being (Wall and Six, 2015). However, 33 % of land is moderately to highly degraded globally, and soil acidification is one of the most important threats to soil's function to support crop production, ranking fourth in the global soil degradation processes (FAO and ITPS, 2015). Soil acidification is generally associated with various conditions restricting crop growth such as deficiency of the base cation (BC), calcium (Ca), magnesium (Mg), and potassium (K), and toxicity induced by aluminium (Al) and manganese (Mn) release (Hue et al., 2001; Zhou, 2015). Furthermore, soil acidification enhances cadmium (Cd) bioaccumulation in crops and animals, negatively affecting food quality and human health (De Vries and McLaughlin, 2013; Song et al., 2017).

Causes of soil acidification can be categorised into the following aspects (Rowell and Wild, 1985): (1) natural soil acidification due to leaching of bicarbonate (HCO_3) and organic anions (RCOO); (2) anthropogenic soil acidification due to acidic atmospheric deposition, application of acidifying fertilizers and removal of vegetation. The dissolution of carbonic acid and organic acid releases a proton (H^+) exchanging with BC, which is then leached to the subsoil together with HCO_3 and RCOO by excess precipitation. This natural release of protons is the main contributor to soil acidification in natural forest and grassland soils, especially in humid forested ecosystems (Fujii et al., 2008; Yu, 1988). However, this release of HCO_3 has minor acidifying effects when the pH is lower than 5.6 but greatly acidifies soils when pH values exceed 6.5, in particular when the soils are characterised by i) high soil organic carbon contents, ii) high CO_2 pressure in soil solutions or iii) when the annual precipitation exceeds the mean potential evapotranspiration leading to a large precipitation surplus (Reuss et al., 1987; Slessarev et al., 2016).

Soil acidification is a naturally slow process (Jiang et al., 2011), which has been greatly accelerated by human activities and their impacts, such as acidic atmospheric deposition, inputs of nitrogen fertilizers and nutrient removal by harvested crops. Human-induced emissions of acidifying compounds such as sulphur dioxide (SO_2) and nitrogen oxides (NO_x) greatly increased due to rapid industrial development. Consequently, acidic deposition has become a serious global environmental problem, elevating the acidity of precipitation and acidifying soils and lakes in Europe and North America (Van Breemen et al., 1984). In agricultural systems, the application of ammonium-based fertilizers strongly acidifies soils due to the H^+ release from nitrification, and the leaching of excess nitrogen (as nitrate) together with BC leaching causes a decline in the capacity of soils to buffer acidification. It was observed in the Park Grass Experiment at Rothamsted that ammonium sulphate application caused a rapid decrease in pH, starting in the surface soil but occurring throughout the profile to at least 1 m depth (Goulding, 2016; Johnston et al., 1986). Crops release H^+ to soil solution when absorbing cations more than anions to maintain the inherent charge balance and vice versa. For grain legumes, crop-induced acidity varied from 46 to 177 cmol kg^{-1}, while the acidity production of cereal crops varied from 25 to 76 cmol kg^{-1} (Tang and Rengel, 2003).

Elevated nitrogen (N) fertilization has largely increased food production but has also caused significant soil acidification in Chinese croplands (Guo et al., 2010). A recent study reveals that the proportion of acidic croplands (pH $<$ 6.5) increased from 36 % to 43 % during 1980s–2010s (Zuo et al., 2023). Even if the increase in N fertilizer use stops, soil acidification will lead to a crop yield decline of 16 % in 2050 (Zhu et al., 2018b; Zhu et al., 2020). Zhu et al. (2018a) revealed that the increase in N transformations and crop removal were the most important factors causing soil acidification. However, their study was carried out at the provincial level without field observations to validate it. Moreover, various other studies showed that different land use types have variable soil acidification rates, suggesting that the main drivers of acidification vary per cropland system. For example, Dong et al. (2022) found that upland and orchards acidified much faster than paddy fields in Southern China. Understanding the historical rates and drivers of soil acidification rates in different cropland systems is key to supporting crop- and site-specific decisions on mitigation strategies.

To increase our understanding of acidification drivers of Chinese croplands, we assessed the historical changes in cropland acidification in a typical Chinese county over the period 1985–2019 using the adapted VSD+ model (Bonten et al., 2016; Zeng et al., 2017) and insights coming from systematic soil sampling networks, farm surveys and literature. We first reconstructed the acidification history of croplands at the county level, after which we assessed the changes in drivers of soil acidification in paddy and upland soils over 30 years.

2. Methods

2.1. Site description

The study was carried out in Qiyang, a typical agricultural county of Hunan Province, China (26°02′N–26°51′N, 110°35′E–112°14′E, see Fig. S1). Qiyang has a typical mild and humid subtropical climate with an annual average temperature of 18.5 °C and an annual average precipitation of 1349 mm, unevenly distributed among seasons, over the period 1981–2010 (China Meteorological Data Service Center). The average cropland area during the period 1985–2019 was about 53 thousand hectares, with paddy (rice) as the dominant crop (90 % of the area) and upland crops being cultivated in the remaining area (Fig. S2a). Since 1985, fertilizer use increased by 50 to 100 %, despite small changes in cropland area (Fig. S2b). Intensive cultivation caused a decline in topsoil pH since the 1980s, mostly due to the overuse of N fertilizers (Zhou, 2017).

The soil sampling compaign and farmer surveys covered paddy rice (56 sites, with single or double cultivation per year), citrus (38 sites) and upland crops (57 sites, including maize, soybean, peanut, sweet potato, rapeseed, sesame, watermelon, tea and vegetable, as well as some rotation systems between them, e.g., maize-sweet potato or peanut-rapeseed system). These crops comprise over 90 % of the total sown area according to the Qiyang Statistical Yearbook (hereinafter referred to as Yearbook). The Yearbooks also cover the annual amount of N, phosphorus (P), K and compounded fertilizers applied, crop yields, population, animal numbers (incl. pigs, cattle, sheep and poultry) and cultivated area per crop at the county level. All data sources with their units and spatial resolution are summarised in Table 1. Details of the data pre-processing and derivation of site-specific nutrient fluxes are described below.

Table 1
Data sources used to assess VSD+ model inputs for the investigated 151 cropland sampling sites at a resolution of 2.7 × 2.7 km combined with county data from the Yearbooks in Qiyang.

Input data	Unit[a]	Data source	Spatial resolution[b]
Climate, irrigation and soil properties			
Precipitation	mm yr^{-1}	Climate Research Unit (CRU) dataset	Downscaling from county to 2.7 km × 2.7 km
Sunshine hours	hr yr^{-1}	CRU dataset	Downscaling from county to 2.7 km × 2.7 km
Air temperature	°C	CRU dataset	Downscaling from county to 2.7 km × 2.7 km
Irrigation of paddy	mm yr^{-1}	He et al. (2020)	Downscaling from nation to 2.7 km × 2.7 km
Bulk density	kg m^{-3}	Harmonized World Soil Data (HWSD) dataset	Upscaling from 1 km × 1 km to 2.7 km × 2.7 km
Clay content	%	HWSD dataset	Upscaling from 1 km × 1 km to 2.7 km × 2.7 km
Sand content	%	HWSD dataset	Upscaling from 1 km × 1 km to 2.7 km × 2.7 km
Initial C:N ratio in soil	g g^{-1}	World Soil Grid	Upscaling from 1 km × 1 km to 2.7 km × 2.7 km
Soil thickness	m	Soil sampling data in 2014 and 2019	2.7 km × 2.7 km
Soil organic carbon content	g kg^{-1}	Soil sampling data in 2014 and 2019	2.7 km × 2.7 km
Soil cation exchange capacity	meq kg^{-1}	Soil sampling data in 2014 and 2019	2.7 km × 2.7 km
Soil base saturation	%	Soil sampling data in 2014 and 2019	2.7 km × 2.7 km
Soil pH	–	Soil sampling data in 2014 and 2019	2.7 km × 2.7 km
Soil $CaCO_3$ content	%	Soil sampling data in 2019	2.7 km × 2.7 km
Soil weathering rates of base cations	keq ha^{-1} yr^{-1}	Model calibration	
Partial CO_2 pressure in the soil solution	mbar	Model calibration	
Nutrient input and outputs			
Atmospheric deposition	kg ha^{-1}	Literature review (see main text)	Downscaling from region to 2.7 km × 2.7 km
N, P, K mineral fertilizer input			
- Total amount of input	kg ha^{-1} yr^{-1}	Yearbooks (1985–2019); farmer surveys (2014)[c]	2.7 km × 2.7 km, annual changes downscaled from county
- Fertilizer type and composition		Yearbooks (1985–2019); farmer surveys (2014)[c]	2.7 km × 2.7 km, annual changes downscaled from county
Organic manure input			
- Application amount	kg ha^{-1} yr^{-1}	Yearbooks (1985–2019); farmer surveys (2014)[c]	2.7 km × 2.7 km, annual changes downscaled from county
- Nutrient content in manure	%	Literature review (see Table S5)	Downscaling from nation to 2.7 km × 2.7 km
Biological N fixation rates	kg ha^{-1} yr^{-1}	Giller (2001); Herridge et al. (2008)	Downscaling from nation to 2.7 km × 2.7 km
Cumulative NH_3 emission from fertilizer	kg ha^{-1} yr^{-1}	Wang et al. (2021)	Downscaling from nation to 2.7 km × 2.7 km
Nutrient crop uptake			
- Crop yields	t ha^{-1}	Yearbooks (1985–2019); farmer surveys (2014)[c]	2.7 km × 2.7 km, annual changes downscaled from county
- Straw: grain ratio	g g^{-1}	Literature review (see Table S7)	Downscaling from nation to 2.7 km × 2.7 km
- Straw returning rates	%	Farmer surveys (2014)	2.7 km × 2.7 km, assuming constant in 2014–2019
- Element contents in harvest and residue	%	Literature review (see Table S7)	Downscaling from nation to 2.7 km × 2.7 km
Regional assessment			
Arable area for paddy, citrus and upland crops	ha	Yearbooks (1985–2019)	County data, assuming constant after 2020
Total N, P and K input from mineral fertilizer	t	Yearbooks (1985–2019)	County data
Potential nutrients from organic manure			
- Human and animal population	unit	Yearbooks (1985–2019)	County data, assuming constant after 2020
- Excretion rate	kg yr^{-1} $unit^{-1}$		Downscaling from nation to county level
- Nutrient content in excretion	%		Downscaling from nation to county level
Actual nutrient inputs from organic manure	t ha^{-1}	Yearbook (2014) and farmer surveys (2014)	Upscaling from the site level (see Eq. (6))
Recycling ratio of potential organic manure	%	Yearbook (2014) and farmer surveys (2014)	Upscaling from sites, assuming constant in 2014–2019

[a] Element input/output was converted from mass fluxes ($kg \cdot ha^{-1} \cdot yr^{-1}$) to charge-equilibrium fluxes ($eq \cdot m^{-2} \cdot yr^{-1}$) as model input by dividing the mass fluxes by 140, 310, 390, 230 and 355 for the monovalent ion N (NH_4^+ and NO_3^-), P ($H_2PO_4^-$), K^+, Na^+ and Cl^-, respectively, and 160, 200 and 120 for divalent ion S (SO_4^{2-}), Ca^{2+} and Mg^{2+}, respectively.

[b] The national and regional data were downscaled to the survey level (2.7 km × 2.7 km).

[c] The farmer survey data were used to assess the input in the year 2014, while the Yearbook data for 1985–2019 were used to scale that input to other years (see, e.g., Eq. (4) for the mineral fertilizer input).

2.2. Modeling soil acidification

2.2.1. Model description

The VSD+ model (Bonten et al., 2016), is an extension of the VSD model (Posch and Reinds, 2009), which simulates soil acidification processes in a single-soil layer. It includes a set of mass balance and equilibrium equations to simulate changes in soil (solution) chemistry, including changes in soil base saturation (BS) and pH, following inputs of N, P, K, Ca, Mg, sulphur (S), sodium (Na), chloride (Cl) and HCO_3 by (in)organic fertilizers, N fixation and deposition, net uptake by plants, and soil biological and chemical processes controlling the availability and solubility of the nutrients. Net nutrient uptake is derived from annual crop yields multiplied by the elemental contents of harvested biomass. N uptake is divided over ammonium (NH_4) and nitrate (NO_3) assuming preferential uptake of NH_4. The applied fertilizer is assumed to dissolve within a year, implying that the nutrients are available as ionic species. Wet and dry deposition from the atmosphere, weathering and uptake rates are given as annual fluxes. The concentration of HCO_3 is based on an equilibrium with the carbon dioxide (CO_2) pressure in the soil solution.

The release of N from the soil organic N pool is calculated from the turnover of the soil carbon pool using the RothC model equations and fixed C:N ratios for five carbon pools varying in decomposability (Coleman and Jenkinson, 1996). Nitrification and denitrification are modelled as first-order rate processes, being affected by temperature and soil moisture. The reduction functions for mineralization (rf_miR), nitrification (rf_nit) and denitrification (rf_denit) of N, due to temperature and/or soil moisture, were computed with the MetHyd model, a simple capacity-based soil water balance model (Bonten et al., 2016). Soil buffering processes include weathering, cation exchange (Gaines-Thomas or Gapon equations) and dissolution of Al hydroxides according to a gibbsite equilibrium. In this study, cation exchange was modelled using the Gapon equation, in which Ca, Mg and K are summed as BC, thereby neglecting the interaction between Na and the adsorption complex. Leaching fluxes are derived by multiplying water fluxes with dissolved element concentrations. Water fluxes at the bottom of the plough layer (20 cm) were calculated using MetHyd. MetHyd requires daily or monthly data of precipitation, average air temperature, and sunshine hours as input variables, whereas the bulk density, soil organic carbon content (SOC) and texture are used to derive the water-holding capacity of the soil. MetHyd computes daily evapotranspiration and percolation, which were aggregated to annual values for use in VSD+. The latest version of the equations of VSD+ with a description of the model parameters can be found in Xu et al. (2023). In addition to nutrient inputs and uptake, VSD+ requires information on soil properties including the cation exchange capacity (CEC) and base saturation, the CO_2 pressure and the concentration of organic C and N.

2.2.2. Model application

The VSD+ model was applied to a total of 151 cropland sites in Qiyang County using data on soil properties and on nutrient inputs and uptake based on a grid-based soil sampling campaign (2.7 km × 2.7 km) and farmer surveys done in 2014. The soil properties included soil pH, soil organic matter content (SOM), CEC (buffered at pH 7) and BS. The farmer surveys were done to retrieve information on agricultural management and included the field size, cultivation period, fertilization (dose, type), crop yield and straw management (being incorporated or not) for different sites. In 2019, 102 sites were resampled for which the crop cultivation remained constant during 2014–2019. At these sites, the pH, BS, calcium carbonate ($CaCO_3$) content, SOM and CEC were measured.

The VSD+ model was initialized in 1985 and the pH changes were simulated for 151 sites up to 2019, using observations of pH changes in 69 non-calcareous soils between 2014 and 2019 as a plausibility check. Changes in soil pH of calcareous soils are negligible due to the high buffering capacity of those soils (Zhu et al., 2018b).

2.2.3. Model calibration and evaluation

Changes in soil pH and BS are mainly affected by the (i) maximum nitrification (knit) and denitrification (kdenit) rate constants, which strongly influence the acidity production by N transformations, (ii) the selectivity constants for H/BC exchange (KHBC), Al/BC exchange (KAlBC) and Al hydroxide dissolution (KAlox), which mainly determine the acid buffering rate, (iii) the partial CO_2 pressure in the soil solution affecting HCO_3 leaching (Xu et al., 2022), and (iv) the BC weathering rates in soil. These constants were initialized based on a plausible range in literature (De Vries and Posch, 2003; Duan et al., 2015; Reinds et al., 2008; Reinds and de Vries, 2010) and further calibrated to minimize the differences between simulated and observed pH and BS values (in 2014 and 2019) measured in the non-calcareous soils using both the Normalized Mean Absolute Error (NMAE) and the Normalized Root Mean Square Error (NRMSE) according to Janssen and Heuberger (1995). Prior distributions of the parameters before calibration are shown in Table S1.

The ranges in maximum nitrification (knit) and denitrification (kdenit) rate constants in VSD+, which are based on data for NH_4:NO_3 concentrations in forest soils in response to N deposition, were adapted for croplands based on literature data. We assumed that 30 % of the total N inputs from fertilizer and manure were denitrified in paddy soils, 5 % higher than the averaged emission in upland soils (Ding et al., 2020; Gu et al., 2015). This was achieved by modifying the maximal denitrification rate (kdenit) to 8.0 (yr^{-1}) for paddy soils while keeping the default value of 4.0 (yr^{-1}) in VSD+ for upland soils. The default range of knit from 0.1 to 4.0 (yr^{-1}) in VSD+ was adapted to 0.45–4.0 in upland soils and from 0.1 to 0.4 in paddy soils, considering that the ratio of NH_4:NO_3 concentrations in soil solution is at a maximum of 1.0 in upland soils (Cai et al., 2014) and on average 2:1 in paddy soils (Sahrawat, 1982).

Both calibration and simulation were done for paddy rice and upland crops separately considering the differences in irrigation rate and partial CO_2 pressure in the soil solution while accounting for soil texture class (distinguishing three categories: sand, moderate clay and heavy clay soils). Soil weathering rates of BC were assumed to vary between 0.5 and 2.0 keq ha^{-1} yr^{-1} for all soil types (Duan et al., 2015). CO_2 pressure varied from 5 to 25 mbar for upland soils (De Vries and Breeuwsma, 1986) and from 25 to 50 mbar for paddy soils (Greenway et al., 2006).

2.2.4. Acidity budget calculations

We calculated the acidity budgets for all sites to identify the key processes contributing to soil acidification by aggregating the various H^+ production and consumption processes (De Vries and Breeuwsma, 1987; De Vries et al., 1989) by procedures outlined in Zeng et al. (2017) and Xu et al. (2023). The total H^+ production (H_{pro}) was calculated as the sum of N transformations, net HCO_3 leaching, crop removal of BC, sulphate ion (SO_4), dihydrogen phosphate (H_2PO_4) and Cl and the net H^+ input, neglecting the difference between the input and output of *RCOO* being minor in croplands (Xu et al., 2023):

$$H_{pro} = (NH_{4in} - NH_{4out} + NO_{3out} - NO_{3in}) + (HCO_{3out} - HCO_{3in}) + \left(BC_{upt} - SO_{4upt} - H_2PO_{4upt} - Cl_{upt}\right) + (H_{in} - H_{out}) \quad (1)$$

where X_{in} is the input of element X (e.g., NH_4, NO_3, HCO_3, *RCOO* and H) from atmospheric deposition and fertilization, X_{upt} represents the element uptake by the crop and X_{out} represents the amount leached out of the soil, determined by VSD+. Note that H^+ consumption occurs when HCO_{3in} is higher than HCO_{3out} which happens when alkaline elements (i.e., atmospheric deposition, fertilizers, lime) are added in excess of acid anions. There is proton consumption when H_{in} is less than H_{out}, which can happen when soil pH is lower than the pH of rainfall. Note that we neglected H_{in} in mineral fertilizers and manure, considering their high pH.

The element output of bicarbonate (HCO_{3out}) was derived by the VSD+ model while HCO_{3in} was calculated based on the charge balance principle:

$$HCO_{3in} = H_{in} + NH_{4in} + BC_{in} + Al_{in} - SO_{4in} - H_2PO_{4in} - Cl_{in} - NO_{3in} \quad (2)$$

We assessed HCO_{3out} and HCO_{3in} separately to quantify the effects of natural acidification and the mitigation effects of alkaline element inputs.

Total H^+ consumption including SO_4 and H_2PO_4 adsorption, as well as BC and Al release was calculated according to:

$$H_{con} = \left(SO_{4in} - SO_{4upt} - SO_{4out}\right) + \left(H_2PO_{4in} - H_2PO_{4upt} - H_2PO_{4out}\right) + \left(BC_{upt} + BC_{out} - BC_{in}\right) + \left(Al_{out} - Al_{in}\right) \quad (3)$$

Note that BC input includes both external inputs (e.g., fertilizers, manure, deposition) and soil BC weathering.

2.3. Data collection

2.3.1. Trends in nutrient inputs from mineral fertilizers

The annual nutrient input from mineral fertilizers between 1985 and

2019 at each cropland site was calculated using 1) the survey data on fertilization rates and fertilizer type in 2014; 2) the Yearbook data on total fertilization rate of N, P and K as well as the total sown area of surveyed crops of the whole county and 3) historical fertilizer type changes estimated from the literature.

Firstly, we checked the plausibility of the survey data based on the Yearbook records in 2014 (Table S2). Overall, the estimated total N inputs based on the farmer surveys were comparable with the Yearbook records in 2014. However, total P and K input showed high variations, most likely due to the overuse of P and K in surveyed sites for double rice and vegetables given the much smaller surveyed area compared to the county-sown area.

Secondly, considering the historical changes in total N, P and K inputs (Fig. S2b), we estimated historical changes in N, P and K input from mineral fertilizers per crop in the various years (1985–2019) based on the survey data and Yearbook records on total fertilizer consumption and sown area in the whole county according to:

$$HFIC_{i,j,k} = SFIC_{j,k} \times \frac{CFI_i \times \sum(SFIC_j \times A_{2014,j})}{CFI_{2014} \times \sum(SFIC_j \times A_{i,j})} \quad (4)$$

where *i*, *j* and *k* are the year, crop and nutrient (N, P or K), respectively. *SFIC* was the surveyed average fertilizer input rate per crop per hectare (kg ha^{-1}) in 2014, *A* was the sowing area of the crop recorded in Yearbook (ha), *CFI* was the county fertilizer input recorded in Yearbook (kg), and *HFIC* was the historical annually-applied fertilizer input rate per crop (kg ha^{-1}) considering the changes in both total fertilizer consumption and sown area during 1985–2019.

Thirdly, we also considered changes in N and P fertilizer types (Fig. S3). According to the farmer surveys, the main fertilizer types were urea and ammonium bicarbonate (NH_4HCO_3) for N, single superphosphate ($Ca(H_2PO_4)_2$) for P, potassium chloride (KCl) for K and N-P-K compound fertilizers (Xu et al., 2022). We then assumed that all applied compound fertilizers were a mixture of urea, ammonium phosphate ($NH_4H_2PO_4$) and potassium chloride (KCl). As a result, 87 % of N inputs were from urea (assuming 50 % NH_4 and 50 % NO_3, see Zeng et al. (2017)), 4.1 % from NH_4HCO_3 and 8.8 % from $NH_4H_2PO_4$. For P inputs, 72 % of them are accompanied with NH_4 and 28 % with Ca. All K was assumed from KCl. These results were quite comparable with the use of fertilizers in China summarised by Zhu et al. (2018a). We then assumed the proportion of N and P fertilizers equal to those at the national level in 1985 where 45 % of N was applied as urea and 55 % as NH_4HCO_3. Similarly, 78 % of P was applied as $Ca(H_2PO_4)_2$ and 22 % as fused magnesium phosphate (FMP). These ratios linearly changed until 2014 indicated by survey results and kept constant after then. As a result, estimated changes in the amount of N fertilizers well fitted historical records by the Yearbooks during 1991–2002 (Fig. S3). The ratios from 1985 to 2019 were then applied to all survey sites to reflect historical fertilizer type changes.

2.3.2. Trends in carbon and nutrient inputs from organic manure

Carbon and nutrient (i.e., N, P, K, Ca, Mg, Na, S and Cl) inputs by organic manure at each cropland site in 2014 were calculated by multiplying the manure application rates based on farmer surveys data with element concentrations in the manure according to National Agro-tech Extension & Service Center (NATESC) records of organic nutrients in China (NATESC,1999). Historical nutrient inputs from organic manure were estimated based on 1) current nutrient inputs from organic manure estimated from the survey data per site in 2014, 2) potential nutrients from organic manure estimated by the Yearbook data on total human and animal population (Fig. S4a) and 3) changes in recycling ratio of nutrients from organic manure from the literature.

Unlike mineral fertilizers, organic manure was not applied per crop but per site annually even though there were multiple crops rotated within one year. Therefore, we firstly calculated the nutrient inputs from organic manure per site (*SMNI*) with one or multiple crop types by multiplying the surveyed manure inputs (*SMI*, t ha^{-1}) by the nutrient content:

$$SMNI_X = \sum_m (SMI_m \times [X]_m) \quad (5)$$

where *m* is the manure type (e.g., pig manure, poultry manure etc., which was only regarded as faeces), [*X*] is the concentration of nutrient *X* (N, P, K etc.) in organic manure. We assumed all carbon and 35 % of the total N input from manure was input directly to the soil pool (the part that did not mineralize during the year of application), as inputs for the RothC model (Xu et al., 2023). The carbon input was determined based on N input and C:N ratio of manure. We assumed the average C:N ratio for animal manure was 15 according to Liu et al. (2023). The mean values are based on 87 publications in which at least 30 % of the data came from China; the C:N ratio for human manure was 25, being the average value of the treated human excretion according to Kelova et al. (2021).

The site-specific nutrient inputs from organic manure were summed up after categorizing into three crop groups: paddy rice, citrus and upland crops (including maize, sweet potato etc.), the total area of which in the county was also given by Yearbooks. Total inputs of nutrients from organic manure for each crop group (*CMNI*) were calculated by summing the nutrient inputs from all sites ($SMNI_X$) under the same crop group. At the county level, actual nutrient inputs from organic manure (*AMNI*) were estimated by multiplying *CMNI*, with the ratio of the total area and the surveyed area of each crop group (*l*) in the region:

$$AMNI_X = \sum_l \left(CMNI_{X,l} \times \frac{TA_l}{SA_l} \right) \quad (6)$$

where *TA* and *SA* are the total area at the county level and correspondingly surveyed area (ha), respectively, of the crop group. These evaluations were carried out by separating calcareous and non-calcareous soils (see Section 2.3.6 Soil properties), excluding 4 extremely large farms, to upscale results to the county level (results of *CMNI* in Table S3 and details in Text S1).

Trends in carbon and nutrient inputs from organic manure over the period 1985–2019 were derived by calculating the potential amount for each year multiplied by historic recycling ratios of organic manure in Qiyang County. Lastly, we assumed the historical nutrient inputs from organic manure per site during 1985–2019 based on the surveyed nutrient inputs in 2014, potential nutrients from organic manure and the recycling ratio of nutrients (*recy_ratio*) during 1985–2019:

$$HMNI_{X,i} = SMNI_X \times \frac{(PAMN_{X,i} + PHMN_{X,i}) \times recy\_ratio_{X,i}}{AMNI_X} \quad (7)$$

where *X* is the nutrient, *i* is the year, *HMNI* is the historical nutrient input rate from organic manure per site, *SNMI* is the surveyed manure inputs in 2014, *PAMN* is the potential animal manure nutrient input at the county level and *recy_ratio* is the recycling ratio of nutrients at the county level.

We assessed potential nutrient inputs from organic manure at the county level considering available human waste and animal manure while distinguishing between the solid part (faeces) and liquid part (urine) of human excreta, pig manure, sheep manure, poultry manure and cattle manure. Available animal manure amounts were estimated based on the number of livestock in the region and the breeding days per cycle, together with the amount of urine and faeces produced per animal. Potential animal manure nutrient inputs (*PAMN*) including (N, P, K, Ca, Mg, S, Na and Cl) were thus calculated as:

$$PAMN_X = \sum_j \left[L_j \times T_j \times \left([X]_{AU,j} \times AUR_j + [X]_{AF,j} \times AFR_j \right) \times (1 - f_{X,j}) \right] \quad (8)$$

where *X* is the nutrient type (N, P, K, Ca, Mg, S, Na and Cl), *j* is animal

type (e.g., pig, sheep, poultry, beef cattle and dairy/farm cattle); L and T are the number of livestock and the breeding days per cycle; AUR and AFR denote the animal urination rate (liquid manure) and defecation rate (solid manure) per day, respectively, and $[X]_{AU}$ and $[X]_{AF}$ are the nutrient X concentrations in animal urine and faeces, respectively; f is the nutrient loss fraction during composting. Breeding cycles and dejection rates of different animals and the element concentrations of urine and faeces were derived from the literature given in Tables S4 and S5, respectively. The nutrient loss fraction for N ($f_{N,j}$) in Eq. (8) was set at 0.2 and 0 for other nutrients according to Bai et al. (2016).

The nutrient inputs from human manure (X_{HM}) were calculated as:

$$PHMN_X = P \times \left([X]_{HU} \times HUR + [X]_{HF} \times HDR\right) \times \left(1 - f_{X,h}\right) \quad (9)$$

where P denotes the human population, HUR and HDR denote the human urination rate (liquid manure) and defecation rate (solid manure) per year; $[X]_{HU}$ and $[X]_{HF}$ denote the nutrient X (N, P, K, Ca, Mg, S, Na and Cl) concentrations in human urine and faeces, respectively, f is the nutrient loss fraction during composting. In this study, the human population and livestock amount were derived from the Yearbook. We assumed that human urination and defecation rates were 550 kg and 51 kg per year, respectively, based on Jönsson et al. (2004). As with animal manure, the nutrient loss fraction for N ($f_{N,h}$) in Eq. (9) was set at 0.2 for N and 0 for other nutrients.

The recycling ratio of nutrients from organic manure in Qiyang County for the year 2014 was calculated as the ratio of the actual amount of nutrients applied in that year, based on the farmer surveys by dividing actual nutrient inputs from organic manure($AMNI_X$) by the potential nutrient inputs from organic manure ($PAMN_X + PHMN_X$) in 2014. Actual applied amounts of nutrients from organic manure on different crops thus derived were 2280 t N, 902 t P and 1752 t K, representing 24 % of N, 34 % of P and 33 % of K in the total human and animal nutrient excretion in Qiyang County (Table S6). These ratios are in plausible ranges considering that 72 % of N, 50 % of P and 48 % of K in manure excretion were lost by housing, storage and treatment losses, as well as discharge (assuming minor grazing losses) in China according to Bai et al. (2016). The historic manure recycling ratios over the period 1985–2014 were based on an assumed decline rate of approximately 0.3 % per year reported by Li et al. (2013). Using a recycling ratio for 2014 of 30 % (mean of N, P and K) led to a recycling ratio of 41 % in 1985 which declined to 30 % in 2014, while it was kept constant at 30 % for the period 2014–2019. Over the past 34 years, the amount of potential nutrients from organic manure constantly increased while the recycling ratio decreased (Fig. S4c).

2.3.3. Carbon inputs from crop straw and roots

The annual C input (t ha^{-1}) by crop straw and crop root input was calculated according to Zhao et al. (2018), by:

$$C_{input} = Yield \times (1 - WC) \times SGratio \times (RSratio + RR) \times 0.45 \quad (10)$$

where $Yield$ is the crop yield (t ha^{-1}), WC is water content as a fraction of the crop (ranging from 0 to 1), $SGratio$ and $RSratio$ is the straw:grain and root:straw ratio of the crop, respectively, RR is the returning ratio of crop straw, and 0.45 is the conversion factor used to convert crop biomass to carbon content (Fang et al., 2007). WC, $GSratio$ and $RSratio$ of different crops are given in Table S7.

2.3.4. Atmospheric deposition, N fixation and ammonia emissions

Historical atmospheric deposition onto Qiyang County during 1985–2019 was based on data from the Qiyang long-term experiment site (1990–2018) in a previous study (Xu et al., 2023), neglecting its spatial variations across Qiyang County. The depositions for 1985–1989 were assumed equal to those in 1990.

The N fixation rates depend on the crop types. For oilseed legumes (soybean and peanut), N fixation was estimated based on the dry weight of grain yield (DW_g, kg ha^{-1}) according to Herridge et al. (2008):

$$N_{fix} = \frac{DW_g}{ind_g} \times N\% \times ind_c \times N_{da} \quad (11)$$

where ind_g is the grain dry matter as a proportion of total above-ground dry matter (set at 40 %); $N\%$ is the average N content of total above-ground parts, which is 3.0 % for soybean and 2.3 % for peanut; ind_c is a multiplier to account for below-ground N, being 1.5 for soybean and 1.4 for peanut, and N_{da} is the ratio of fixed N divided by N content of crop (set at 50 %). For paddy rice and other upland crops, we assumed a N fixation rate of 30 and 5 kg ha^{-1} yr^{-1}, according to Giller (2001) and Herridge et al. (2008), respectively. Nutrient inputs from irrigation and seeds were neglected.

Emission of NH_3 was assessed based on an empirical model for Chinese croplands (Wang et al., 2021), considering the effects of N fertilizer input rate and type (e.g., mineral fertilizer only, organic fertilizer only or mixture of them), soil clay content and air temperature. The cumulative NH_3 emission rate (kg ha^{-1} yr^{-1}) per site was calculated by:

$$Cum\_NH_3 = exp\left(-1.612 + 0.007 \cdot N_{rate} + 0.043 \cdot clay + 0.038 \cdot Tem + cof_{fer}\right) \quad (12)$$

where N_{rate} is N application rate (kg ha^{-1} yr^{-1}), $clay$ is soil clay content (%), Tem is air temperature (°C), cof_{fer} is coefficients for fertilizer type, which is 0.94 for mineral fertilizers, 1.36 for organic fertilizers and 0.90 for any mixture of them, respectively. Site-specific N input rate and type were derived from farmer surveys, and soil clay content was derived from existing databases (see details below).

2.3.5. Element removal by crops

Element removal during 1985–2019 for the 151 sites was estimated from harvested crop yield (CY) and crop residues by multiplying the crop yields (including residues) by mineral contents summarised by Zhu et al. (2018a). Historical crop yields were derived by using the measured crop yield from the farmer surveys for the year 2014 and superimposing the changes in time for each crop, calculated by dividing the annual total yield and sown area (under cultivation used for cropping) recorded in the Yearbook (Fig. S5) according to:

$$CY_{i,j} = SY_j \times \frac{TY_{i,j}/A_{i,j}}{TY_{2014,j}/A_{2014,j}} \quad (13)$$

where i and j is the year and crop, respectively. SY is the surveyed yield per crop in 2014, TY is the total crop yield, and A is the sowing area of the crop recorded in the Yearbook. We thus assumed that the average crop yield change over the years holds for all sites.

Crop residue removal rates were calculated by multiplying the crop yield with the straw:grain ratio and straw removal ratio. The removal ratio was assumed 100 % if the farmers indicated that they removed residues. According to the survey, the current straw returning rate for paddy rice, upland crops and citrus is on average 84 %, 40 % and 5 %, respectively (Table S8). Given the historical crop residue returning ratio changed, we assumed that in the year 1985 crop residue returning ratio was 30 % for all crops (Zhu et al., 2018a), after which the ratio is assumed to increase linearly up to 84 % for rice and 40 % for all other upland crops in 2014, after which the ratio was kept constant until 2019. For citrus, the historical changes in residue returning were neglected. The straw:grain ratio, N, P, K, Ca, Mg, S and Cl contents (%) in grain and straw (branches) for typical crops and fruits in Qiyang were derived from the literature (see Table S7).

2.3.6. Soil properties

Soil properties in 1985 were used as initial inputs for the VSD+ model. Initial soil pH, SOC and total N were derived from Qiyang Soil Species Records (Soils of Qiyang County, Qiyang County Land Management Bureau, Qiyang, 1991) based on the Second National Soil

Survey of China in the 1980s. As the 98 sites from the 1980s period were not georeferenced, we manually determined the location based on soil type and town (village) name. The soil properties were rasterized using inverse distance weighting (IDW) interpolation after which the relevant soil properties on the survey sites were extracted using a spatial intersection. Initial BS was derived based on a linear pH-BS relationship up to a pH of 6.5 after which we assume a BS of 100 % (see Xu et al., 2022). Other soil properties, including bulk density, CEC and soil texture (clay and sand content), were derived from the 1 × 1 km^2 Harmonized World Soil Data map (HWSD) version 1.1 (Fischer et al., 2008) whereas the C:N ratio was retrieved from the World Soil Grid data (Hengl et al., 2017; Poggio et al., 2021). In 2014 and 2019 soil pH, SOM, CEC, BS and soil calcium carbonate content ($CaCO_3$) were measured ($CaCO_3$ in 2019 only). As CEC does not change in VSD+, we used the mean value of the measured CEC as the initial input. Missing soil data on soil pH and BS in 2019 were estimated based on the data in 2014 and the average trends in those soil data at the sites with paired data in both 2014 and 2019 (see Text S2 and Fig. S6). The measured $CaCO_3$ content in 2019 was used to assess whether the soils were calcareous or non-calcareous, and when carbonate observations were missing, soils with pH in 2014 higher than 7.0 were assumed to be calcareous. As a result, 69 survey sites were located on non-calcareous soils, representing 48 % of the total survey area.

2.3.7. Meteorology and hydrology

Daily climate data were taken from observations at a long-term experiment in Qiyang, while variations over the Qiyang County were derived by scaling the daily values to variation in monthly mean values at 10 min resolution from the Climate Research Unit (CRU) (New et al., 2002). This database contains gridded data on temperature and precipitation, vapour pressure, cloud cover and wet-day frequency in terms of rain day counts at the global scale at 10 min resolution, averaged over the reference 30-year period 1961–1990 (mean monthly values and the coefficient of variation shown in Table S9 and spatial distribution shown in Fig. S7). For irrigation rate, we assumed an average rate of 840 mm yr^{-1} (12 × 70 mm per month) in paddy based on He et al. (2020), and no irrigation for upland crops (rainfed only).

Using a simple uncertainty analysis on the calculated water fluxes from MetHyd showed that land use (paddy and upland soils) and soil texture (sandy, moderate clay and heavy clay soils) had a strong and significant effect on the estimated leaching, whereas spatial variations in climate conditions (across all survey sites) had minor effects (see details in Text S3). Therefore, we divided all sites into 6 groups (2 types of land use × 3 types of soil texture) and used mean values of the MetHyd output for the modeling of soil acidification (see outcomes of precipitation surplus in Table S10).

3. Results

3.1. Reconstruction of acidification history

The VSD+ model well reconstructed the continuous soil acidification in non-calcareous croplands of Qiyang County during 1985–2019 (Fig. 1). On average, the simulated soil pH declined from 6.2 to 5.4 in paddy soils and from 6.2 to 5.2 in upland soils, with annual pH decline rates of 0.024 and 0.029 units yr^{-1}, respectively. Even though the observed decline in soil pH was slightly higher in upland soils, the difference in the annual pH decline rate was not statistically significant ($P > 0.05$). In general, the pH of paddy soils showed smaller variations than upland soils over the simulation period. The base saturation followed a similar decreasing trend as pH and declined by 0.96 % per year (from 84 % to 53 %) in paddy soils and by 1.1 % per year (from 80 % to 44 %) in upland soils. On average, base saturation declined faster before the year 2000 in both paddy and upland soils than in the years thereafter. Again, differences between paddy and upland soils were not statistically significant ($P > 0.05$) (Fig. 1). VSD+ slightly underestimated the soil pH and BS before 2014, particularly in paddy soils, while the variation across sites was comparable (Fig. 1). For calcareous soils, the pH of both

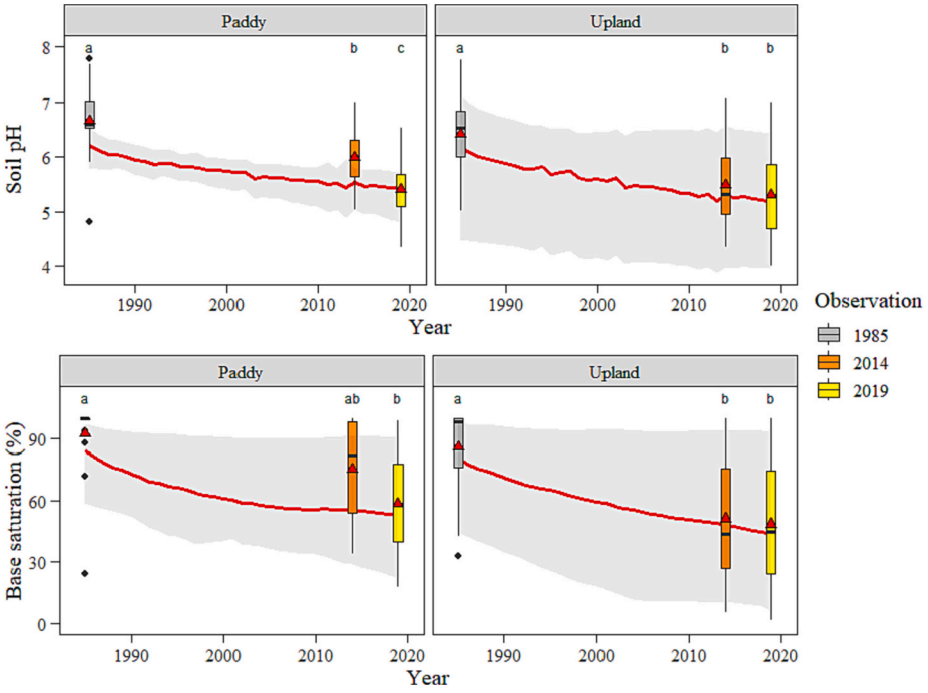

Fig. 1. Historical soil pH (top) and base saturation (bottom) change over the period 1985–2019 in non-calcareous paddy soils (left) and upland soils (right) of Qiyang County. Red lines indicate the mean of simulations; the grey areas represent the range in the 5 % and 95 % percentile of the simulation. Boxes represent observations, with the bias being 5 % and 95 % percentile of data, triangles and lines in the boxes indicate mean and median values, respectively. Different letters above the bars indicate the observations have significant differences ($p < 0.05$, Tukey method for multiple comparisons) among different years for same land use type (paddy and upland).

paddy soils and upland soils kept stable over the 34 years (Fig. S8).

The cumulative frequency of soil pH showed that the average deviation between simulated and observed pH values was low for most crop categories, as shown by the NRMSE (0.06–0.15) and NMAE (0.07–0.12) over the whole observation period (Fig. 2). In the year 1985, over 90 % of paddy soils and 80 % of upland soils had pH values > 5.5, while the percentage of soils with pH > 5.5 gradually declined to around 50 % in 2019 in both paddy soils and upland soils, implying that a considerable proportion of croplands are currently facing acidity threats and associated adverse impacts on soil health and crop production.

3.2. Reconstruction of soil acidification rates and main drivers

The 5-year-average H^+ production considerably declined in paddy soils from 21 to 5.2 keq ha^{-1} yr^{-1} during 1985–2019 (Fig. 3), which was mostly due to the great decline in HCO_3 leaching and N transformations. In contrast, the total soil acidification rate in upland soils hardly changed, decreasing from 17 to 13 keq ha^{-1} yr^{-1}, mostly driven by N transformations, while crop-induced H^+ production slightly increased. Both HCO_3 input and BC release dominated the H^+ consumption processes in paddy and upland soils. HCO_3 input strongly declined after 2005 in paddy soils while it remained relatively constant in upland soils. BC release strongly decreased in paddy soils while it hardly changed in upland soils. Aluminium release considerably contributed to H^+ consumption in upland soils after 2005 when the soil pH was lower than 5.5. The P adsorption increased in both paddy and upland soils.

Paddy soils had lower N transformations than upland soils, despite much higher NH_4 inputs (indicating higher potential acidification) from mineral fertilizer (for details of the N budgets, see Table 2). This was mainly due to: 1) higher crop nutrient uptake and lower N leaching losses; 2) higher denitrification losses; and 3) lower nitrification rates as the NH_4/NO_3 ratio in soil solution was much higher. Changes in P fluxes mainly originated from an increase in P fertilizer inputs (Fig. 4a). In addition, total BC inputs increased both in paddy and upland soils, whereas the uptake and losses slightly decreased in paddy soils, leading to much less BC release compared to the upland soils where the BC uptake increased over time (Fig. 4b). The decline in HCO_3 inputs originates from a change in mineral fertilizer types where NH_4HCO_3 fertilizers have been replaced with urea (Fig. S3). This decline in upland soils was counteracted by the increase in HCO_3 inputs in organic manure (Fig. 4c). Note also the HCO_3 input in deposition, which was due to an excess of the sum of NH_4 and BC over anions (SO_4, H_2PO_4, Cl and NO_3) (Xue et al., 2003; Zeng et al., 2017).

Over the past 34 years, HCO_3 leaching and N transformations were the dominant processes driving soil acidification in non-calcareous paddy soils (no significant difference) whereas N transformations was the main driver of soil acidification in non-calcareous upland soils (Fig. 5a). HCO_3 input was the main H^+ consumption process, followed by BC and Al release in non-calcareous soils. In calcareous soils, HCO_3 leaching played dominant role in H^+ production in both paddy soils and

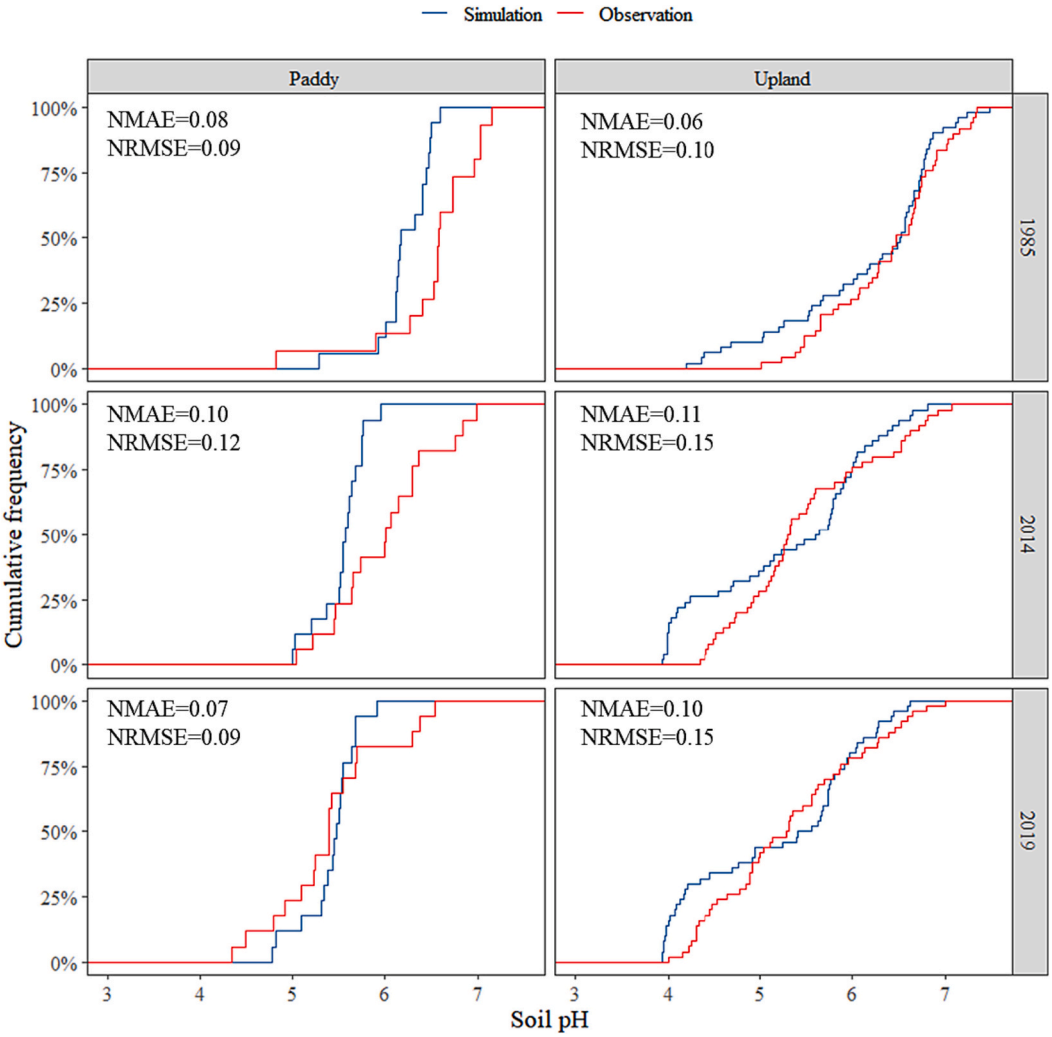

Fig. 2. Cumulative frequency of simulated and observed soil pH in non-calcareous paddy soils (left) and upland soils (right) in 1985 (top), 2014(center) and 2019 (bottom).

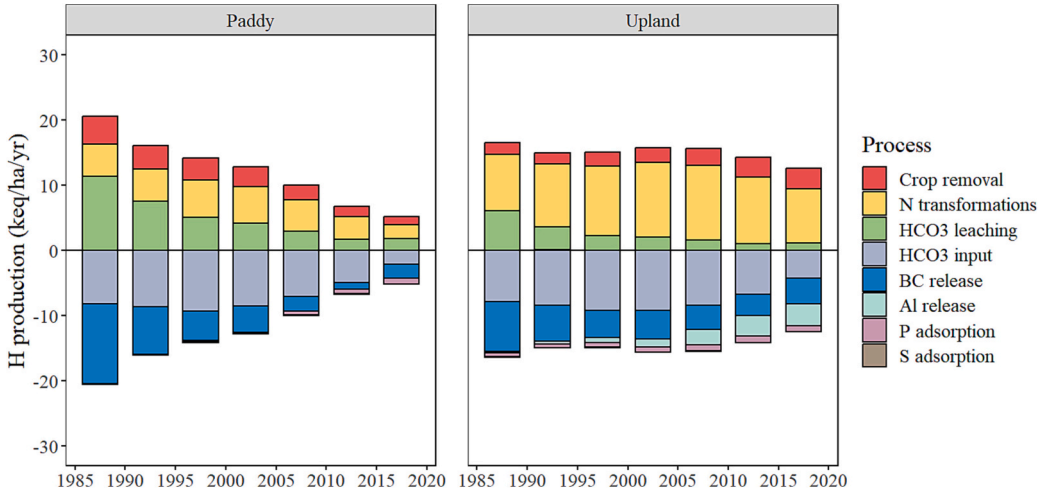

Fig. 3. Historical average H production (positive values) and consumption (negative values) (keq ha^{-1} yr^{-1}) every 5 years in paddy soil (left) and upland soils (right) in non-calcareous sites of Qiyang County (1985–2019). Note that net HCO_3 leaching is split into HCO_3 leaching (natural acidification) and HCO_3 (alkalinity) input from atmospheric deposition, fertilizer and manure. Net H input is too minor to show in the figure.

Table 2
Simulated N budget for paddy and upland soils in non-calcareous sites, averaged over the period 1985–2019.

Flux	Paddy	Upland
Input		
Atmospheric deposition	3.2	3.2
NH_4	2.4	2.4
NO_3	0.8	0.8
Fertilizer	12.7	7.1
NH_4	8.2	4.6
NO_3	4.5	2.5
Manure	0.3	3.3
N fixation	2.1	1.1
Total input	18.3	14.7
Output		
Uptake	10.6	4.8
NH_3 emission	1.5	1.3
Surplus	6.2	8.8
Denitrification[a]	3.9	2.6
NH_4 leaching[a]	2.1	0.9
NO_3 leaching[a]	1.1	5.4
Soil accumulation	−0.9	−0.3

[a] Corrected by N input to soil pool.

upland soils, while BC release played the most important role in H^+ consumption (Fig. 5b).

4. Discussion

4.1. Historic soil pH and base saturation trends

Overall, simulated soil pH fitted well with the mean of observation between 2014 and 2019 in paddy soils, with an averaged decreasing rate of 0.024 units yr^{-1} since 1985. The pH-declining rate in paddy soils is quite comparable with previous studies, e.g., Zhu et al. (2016) reported that the pH of paddy soil in Hunan Province declined by 0.031 units yr^{-1} during 1980s–2014 on average. There was large variability in the observed soil pH, which was measured in a 1:2.5 soil: water suspension, of paddy soils during 2014–2019, which is likely due to variable weather conditions and fertilizer application which may affect pH values by as much as 0.6 units (Shuman et al., 1983; Sumner, 1994).

The average pH decline of upland soils was slightly higher but not statistically different from paddy soils (pH declined by 0.029 units yr^{-1} over the simulation years), though VSD+ slightly underestimated the simulated pH of upland soils during 2014–2019. The uncertainties in the simulations were most likely due to the uncertainties of our estimations on the historical land use. On average, the mean cultivation period of surveyed citrus sites was 15 years (Table S8) indicating that our estimations on element input-output during 1985–2000 based on the survey data may not well reconstruct the historical trends, leading to the uncertainties in calculated soil acidification rates. In addition, there are uncertainties in the (calibrated) parameters affecting the N transformations, crop uptake and HCO_3 leaching rates. The comparable pH declines in paddy and upland soils, despite the lower acidifying impact of N transformations were due to the higher acidifying impact of HCO_3 leaching (Fig. 5a). This was caused by the wetter circumstances in paddy soils, which enhanced denitrification and thus reduced NO_3 leaching and increased the CO_2 pressure of the soil, thus enhancing HCO_3 leaching.

Our results showed that soil pH significantly decline in both paddy soils and upland soils between the year 1985 and 2019 (Fig. 1). In addition, we found a significant difference between soil pH in the year 2014 and 2019 in paddy soils but not in upland soils, which may be caused by the uncertainty in measured pH values (in H_2O) in paddy soils due to the variable soil moisture contents in the different months in which the pH was measured (Ding et al., 2019). Actually, soil pH was measured in June–July in 2014 and in October–November in 2019, probably affecting the comparability of the soil pH measurement.

In our study, NH_3 emissions were estimated considering N input rate, soil clay content, air temperature and fertilizer types. Overall, NH_3 emissions in upland and paddy soils were comparable, ranging between 11.5 and 12.6 % of the total N added. This result was slightly different from previous studies. For instance, Ma et al. (2022) showed that paddy fields tended to have higher background NH_3 emissions compared to upland soils, suggesting that our study may underestimate NH_3 emissions in paddy soils. This underestimation in paddy soils might be caused by the fact that we ignored the influence of application methods due to a lack of reliable data, while NH_3 losses are substantially higher when manure and fertilizers are broadcasted rather than incorporated (Wang et al., 2021).

It should be noted that calibrated model parameters *knit*, *kdenit*, *pCO2*, *lgKAlBC*, *lgKHBC*, *lgKAlox* and *BC* weathering varied quite a lot among the sites (Fig. S9), mostly within plausible ranges (see e.g., De Vries and Posch (2003) for the range in exchange constants). Since these parameter values are not clearly related to soil properties, the application of VSD+ to other regions than Qiyang implies the use of generic model parameters that may cause errors in site-specific acidification assessments.

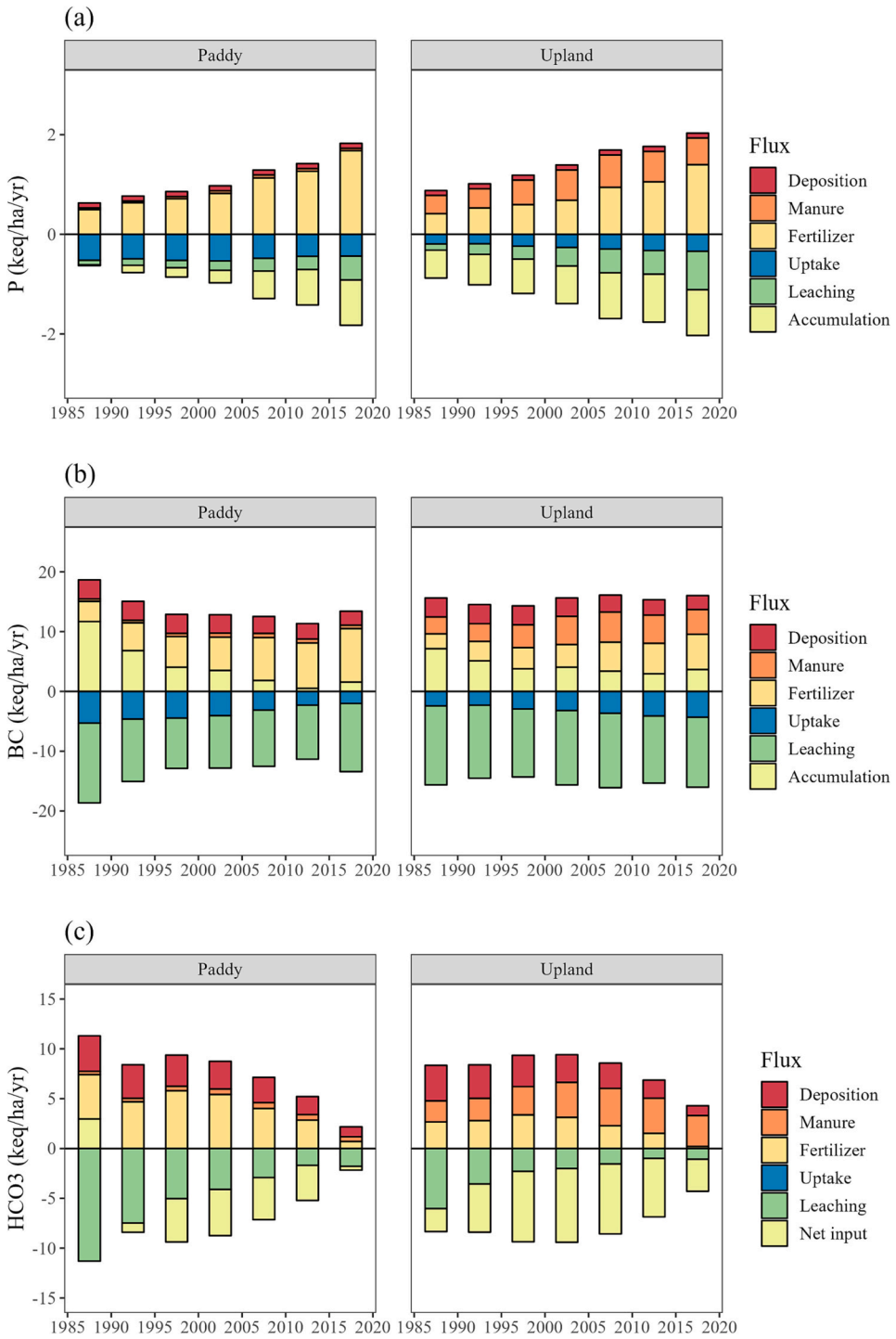

Fig. 4. Historical element input and output (1985–2019, mean of every 5 years) of phosphorus (a), base cations (b) and bicarbonate (c) in non-calcareous sites.

4.2. Soil acidification trends and their main drivers

Significant soil acidification in Chinese croplands has been proven to be induced by the overuse of N fertilizers, and N transformations have been shown to have a major impact on the acidification processes (Guo et al., 2010; Zeng et al., 2017; Zhu et al., 2018a). Our study had the same finding in upland soils but showed that HCO_3 leaching was also the main driver of acidification of paddy soils, mostly due to the elevated CO_2 pressure under the flooding situation. This implies that the reason of soil acidification in paddy soils as well as the appropriate measures to compensate it strongly differ between these cropping systems. Theoretically, an increase in CO_2 pressure from 15 to 100 mbar leads to an increase in HCO_3 concentrations from 2.8 to 5.3 meq L^{-1} in calcareous soils, leading to a net H^+ production increase from 28 to 53 keq ha^{-1} yr^{-1} in calcareous soils. In non-calcareous soils, soil pH also controls the HCO_3 concentration and the impact of a change in the CO_2 pressure. For instance, when soil pH is 5.0, increasing pCO_2 from 15 to 100 mbar would increase HCO_3 concentration from 0.024 to 0.16 meq L^{-1}, whereas the HCO_3 concentration would increase up to 1.6 meq L^{-1} when soil pH is 6.0. According to Greenway et al. (2006), CO_2 pressure in the soil solution of paddy rice could reach as high as 400 mbar.

In paddy fields with a relatively high soil pH and high precipitation

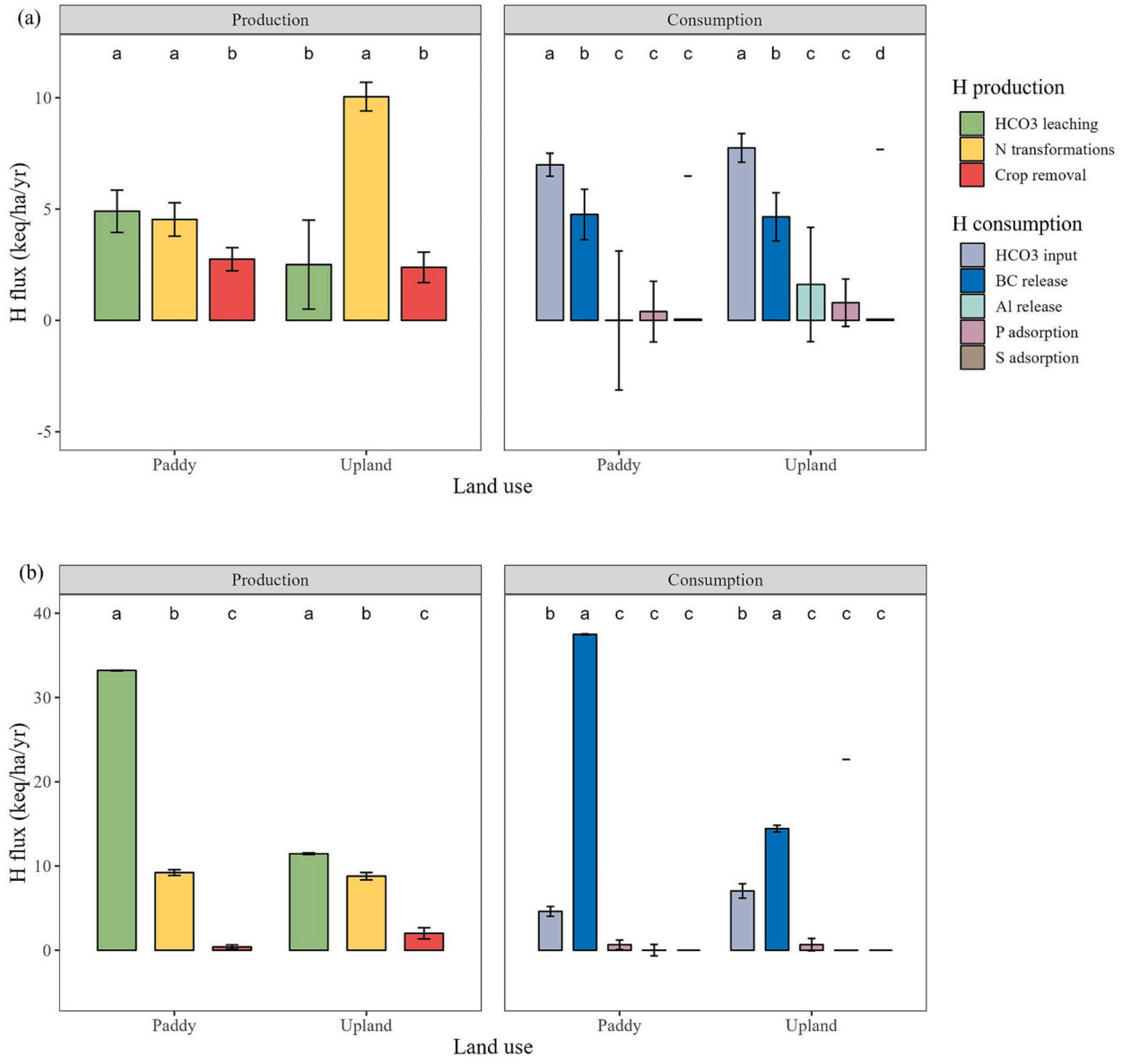

Fig. 5. Contribution of different processes to cropland acidification rates (keq ha^{-1} yr^{-1}) of paddy and upland soil in non-calcareous sites (a) and calcareous sites (b) of Qiyang County averaged over the period 1985–2019 in terms of production (left) and consumption (right). The bar height is the mean value and the error bar is the variation (s.d./mean) over the 34 years. Different letters above the bars indicate the processes have significant differences ($p < 0.05$, Tukey method for multiple comparisons) for same land use type (paddy and upland). Net H input is too minor to show in the graphs.

surplus, net HCO_3 leaching may thus lead to significant soil acidification. China is the world-leading rice production country, with a total area of 30 million hectares of paddy (~20 % of the total cropland area) and >80 % of this area with annual precipitation ranging from 1000 to >2000 mm (Liu et al., 2018). Qiyang is a representative county in the region with an average precipitation surplus of 1400 mm. Our study thus suggests that the acidification rates due to HCO_3 leaching in paddy rice were underestimated in a national study on drivers of soil acidification by Zhu et al. (2018a), who used a precipitation surplus of 100–400 mm. Further studies are required to evaluate the effects of CO_2 pressure and soil pH on HCO_3 leaching based on more evidence in the field.

N transformations were mainly driven by the inputs of mineral fertilizers and organic manure as well as crop nutrient uptake. Before 2005, as the application of N increased (in particular for NH_4), N transformations also increased, followed by a combined decline in the years after 2014 (Fig. 3). The increase in N-induced acidification was mainly due to the enhanced nitrification of NH_4 to NO_3 and subsequent NO_3 leaching. However, the N-induced H^+ production was also highly neutralized by the anthropogenic input of HCO_3 (from NH_4HCO_3 and organic manure), which was the main contributor to the H^+ consumption process between 1990 and 2015. In addition, there was also HCO_3 input in the deposition, since the sum of cations (NH_4, BC) exceeded that of anions (SO_4, H_2PO_4, Cl, NO_3), being in line with other literature information (Xue et al., 2003; Zeng et al., 2017). The NH_3 emission induced by NH_4 input is a potential acid source due to nitrification in soil.

The long-term observations carried out in Qiyang imply that the net impact of N fertilization on soil acidification is easily overestimated when only the impacts on N transformations are included, e.g., by Guo et al. (2010). The overall impact of N fertilizers might even lead to increases in soil pH when N is added as NH_4HCO_3 and a low proportion of added N is lost due to high denitrification. The H^+ production by crop removal was driven by the removed biomass from the field as the crop yield in paddy rice hardly changed over the past 34 years. In upland soils, despite an increasing straw return ratio, the total crop production strongly increased (Fig. S5), leading to an increase in crop-induced H^+

production.

4.3. Implications for soil acidity management

Previously, Zeng et al. (2017) suggested that soil acidity management should focus on optimizing N management and increasing BC inputs by manure application in intensive cropland systems. Our study leads to a similar conclusion for upland soils. N transformations dominated soil acidity production processes in these soils and optimizing N management, e.g., by balancing N input, increasing N use efficiency and transforming ammonium-based fertilizers to urea- or nitrate-based fertilizers, is crucial to mitigate soil acidification. Furthermore, HCO_3 input plays an important role in acidity consumption processes and increasing organic manure input rich in BC and HCO_3 can thus reduce soil acidification rates.

However, for paddy fields, our study shows that the average impacts of HCO_3 leaching on soil acidification was comparable with N transformations, mainly because of the high CO_2 pressure under flooding situations and generally high pH values over the past 30 years in Qiyang County. However, the effects decreased substantially when soil pH declined under 6.0 as the concentration of HCO_3 in soil solution is highly controlled by soil pH. It suggested that acid management in paddy fields requires additional focus on avoiding mitigation strategies that raise the soil pH level >6.0 to avoid unnecessarily high HCO_3 leaching, accelerating soil acidification.

5. Conclusions

In this study, we quantified rates and drivers of soil acidification for paddy and upland soils over the period 1985–2019 at 151 sites in Qiyang, a typical agricultural county in China, with the soil acidification model VSD+. The model was applied and validated using systematic farm surveys in 2014 and soil sampling data for the years 1985 (based on sampling in the 1980s), 2014 and 2019. The VSD+ model could well reproduce long-term changes in pH, showing a pH decline of 0.024 and 0.029 units yr^{-1} in paddy and upland soils, respectively, and declining concentrations of calcium, magnesium and potassium.

Nitrogen (N) transformations mainly caused soil acidification in upland soils, but in paddy soils natural soil acidification due to bicarbonate leaching was also a major driver of acdification. The lower impact of N transformations on soil acidification in paddy soils was due to their wet circumstances, causing higher crop N uptake, lower nitrification rates and higher denitrification rates, thus leading to lower NO_3 leaching losses than in upland soils. Similarly, the wet circumstances caused higher HCO_3 leaching due to a higher CO_2 pressure. However, the contribution of this process decreased due to acidification-induced soil pH decrease.

The acid input from fertilizers and deposition was partly neutralized by HCO_3 input from fertilizers and manure, but this decreased in time in both upland soils and paddy soils due to a change in fertilizer type from ammonia bicarbonate to urea. Base cations removal by crop harvesting played a minor role in both paddy and upland soils, but the relative importance increased in paddy soils due to a decrease in HCO_3 leaching. Soil buffering by both BC and aluminium release decreased in paddy soils due to a reduction in net acid production, while it stayed relatively constant in upland soils, but with an enhanced contribution of aluminium release due to pH decline.

We conclude that acidification management in upland soils requires a focus on balancing N and BC by enhanced recycling of organic manure and crop residues, while the pH in paddy soils should not be brought to a too high level to avoid high HCO_3 leaching. Due to the high CO_2 pressure in those soils, liming strongly induces natural soil acidification and this requires a subtle balance in avoiding both too low and too high pH values.

CRediT authorship contribution statement

Donghao Xu: Writing – original draft, Visualization, Investigation, Formal analysis, Data curation. **Gerard H. Ros:** Writing – review & editing, Visualization, Supervision. **Qichao Zhu:** Supervision, Methodology, Conceptualization. **Minggang Xu:** Writing – review & editing, Resources. **Shilin Wen:** Writing – review & editing, Resources. **Zejiang Cai:** Writing – review & editing, Resources. **Fusuo Zhang:** Supervision, Project administration, Funding acquisition. **Wim de Vries:** Writing – review & editing, Supervision, Project administration, Methodology, Conceptualization.

Declaration of competing interest

The authors declare that they have no known competing financial interests or personal relationships that could have appeared to influence the work reported in this paper.

Data availability

Data will be made available on request.

Acknowledgement

This research is financially supported by National Key Research and Development Program of China (2022YFD1900601), Key R&D Plan of Yunnan Province (202102AE090030), China Scholarship Council (No. 201913043) and Hainan University; we also acknowledge Qiyang Agro-ecosystem of National Field Experimental Station for data support, and Dr. Gert Jan Reinds from Wageningen University & Research for his supports on helping us to use the VSD+ model.

Appendix A. Supplementary data

Supplementary data to this article can be found online at https://doi.org/10.1016/j.scitotenv.2024.170189.

References

Bai, Z., Ma, L., Jin, S., Ma, W., Velthof, G.L., Oenema, O., Liu, L., Chadwick, D., Zhang, F., 2016. Nitrogen, phosphorus, and potassium flows through the manure management chain in China. Environ. Sci. Technol. 50, 13409–13418.

Bonten, L.T.C., Reinds, G.J., Posch, M., 2016. A model to calculate effects of atmospheric deposition on soil acidification, eutrophication and carbon sequestration. Environ. Model Softw. 79, 75–84.

Cai, Z., Wang, B., Xu, M., Zhang, H., Zhang, L., Gao, S., 2014. Nitrification and acidification from urea application in red soil (Ferralic Cambisol) after different long-term fertilization treatments. J. Soils Sediments 14, 1526–1536.

Coleman, K., Jenkinson, D.S., 1996. RothC-26.3 - a model for the turnover of carbon in soil. In: Powlson, D.S., Smith, P., Smith, J.U. (Eds.), Evaluation of Soil Organic Matter Models. Springer Berlin Heidelberg, Berlin, Heidelberg, pp. 237–246.

De Vries, W., Breeuwsma, A., 1986. Relative importance of natural and anthropogenic proton sources in soils in the Netherlands. Water Air Soil Pollut. 28, 173–184.

De Vries, W., Breeuwsma, A., 1987. The relation between soil acidification and element cycling. Water Air Soil Pollut. 35, 293–310.

De Vries, W., McLaughlin, M.J., 2013. Modeling the cadmium balance in Australian agricultural systems in view of potential impacts on food and water quality. Sci. Total Environ. 461–462, 240–257.

De Vries, W., Posch, M., 2003. Derivation of cation exchange constants for sand, loess, clay and peat soils on the basis of field measurements in the Netherlands. In: Alterra-rapport, vol. 701. Alterra Green World Research, Wageningen, the Netherlands (50 pp.).

De Vries, W., Posch, M., Kämäri, J., 1989. Simulation of the long-term soil response to acid deposition in various buffer ranges. Water Air Soil Pollut. 48, 349–390.

Ding, X., Du, S., Ma, Y., Li, X., Zhang, T., Wang, X., 2019. Changes in the pH of paddy soils after flooding and drainage: modeling and validation. Geoderma 337, 511–513.

Ding, W., Xu, X., He, P., Zhang, J., Cui, Z., Zhou, W., 2020. Estimating regional N application rates for rice in China based on target yield, indigenous N supply, and N loss. Environ. Pollut. 263, 114408.

Dong, Y., Yang, J., Zhao, X., Yang, S., Mulder, J., Dörsch, P., Peng, X., Zhang, G., 2022. Soil acidification and loss of base cations in a subtropical agricultural watershed. Sci. Total Environ. 827, 154338.

Duan, L., Zhao, Y., Hao, J., 2015. Critical load assessments for sulphur and nitrogen for soils and surface waters in China. In: Critical Loads and Dynamic Risk Assessments, pp. 419–438.
Fang, J., Guo, Z., Piao, S., Chen, A., 2007. Terrestrial vegetation carbon sinks in China, 1981–2000. Sci. China Ser. D Earth Sci. 50, 1341–1350.
FAO and ITPS, 2015. Status of the world's soil resources (SWSR) – technical summary. In: Food and Agriculture Organization of the UN and Intergovernmental Technical Panel on Soils, Rome, Italy.
Fischer, G.F., Nachtergaele, S., Prieler, H.T., van Velthuizen, L., Verelst, D.W., 2008. Global Agro-ecological Zones Assessment for Agriculture (GAEZ 2008). IIASA Laxenburg, Austria and FAO, Rome, Italy.
Fujii, K., Funakawa, S., Hayakawa, C., Kosaki, T., 2008. Contribution of different proton sources to pedogenetic soil acidification in forested ecosystems in Japan. Geoderma 144, 478–490.
Giller, K., 2001. Nitrogen Fixation in Tropical Cropping Systems. CABI publishing, Wallingford.
Goulding, K.W.T., 2016. Soil acidification and the importance of liming agricultural soils with particular reference to the United Kingdom. Soil Use Manag. 32, 390–399.
Greenway, H., Armstrong, W., Colmer, T.D., 2006. Conditions leading to high CO_2 (>5 kPa) in waterlogged-flooded soils and possible effects on root growth and metabolism. Ann. Bot. 98, 9–32.
Gu, B., Ju, X., Chang, J., Ge, Y., Vitousek, P., 2015. Integrated reactive nitrogen budgets and future trends in China. Proc. Natl. Acad. Sci. U. S. A. 112, 8792–8797.
Guo, J., Liu, X., Zhang, Y., Shen, J., Han, W., Zhang, W., Christie, P., Goulding, K., Vitousek, P., Zhang, F., 2010. Significant acidification in major Chinese croplands. Science 327, 1008–1010.
He, G., Wang, Z., Cui, Z., 2020. Managing irrigation water for sustainable rice production in China. J. Clean. Prod. 245.
Hengl, T., Mendes de Jesus, J., Heuvelink, G.B., Ruiperez Gonzalez, M., Kilibarda, M., Blagotic, A., Shangguan, W., Wright, M.N., Geng, X., Bauer-Marschallinger, B., Guevara, M.A., Vargas, R., MacMillan, R.A., Batjes, N.H., Leenaars, J.G., Ribeiro, E., Wheeler, I., Mantel, S., Kempen, B., 2017. SoilGrids250m: global gridded soil information based on machine learning. PLoS One 12, e0169748.
Herridge, D.F., Peoples, M.B., Boddey, R.M., 2008. Global inputs of biological nitrogen fixation in agricultural systems. Plant Soil 311, 1–18.
Hue, N.V., Vega, S., Silva, J.A., 2001. Manganese toxicity in a Hawaiian Oxisol affected by soil pH and organic amendments. Soil Sci. Soc. Am. J. 65, 153–160.
Janssen, P.H.M., Heuberger, P.S.C., 1995. Calibration of process-oriented models. Ecol. Model. 83, 55–66.
Jiang, J., Xu, R.-k., Zhao, A.-z., 2011. Surface chemical properties and pedogenesis of tropical soils derived from basalts with different ages in Hainan, China. Catena 87, 334–340.
Johnston, A.E., Goulding, K.W.T., Poulton, P.R., 1986. Soil acidification during more than 100 years under permanent grassland and woodland at Rothamsted. Soil Use Manag. 2, 3–10.
Jönsson, H., Stintzing, A.R., Vinnerås, B., Salomon, E., 2004. Guidelines on the Use of Urine and Faeces in Crop Production. EcoSanRes Programme.
Kelova, M.E., Eich-Greatorex, S., Krogstad, T., 2021. Human excreta as a resource in agriculture – Evaluating the fertilizer potential of different composting and fermentation-derived products. Resour. Conserv. Recycl. 175, 105748.
Li, Y., Zhang, W., Ma, L., Huang, G., Oenema, O., Zhang, F., Dou, Z., 2013. An analysis of China's fertilizer policies: impacts on the industry, food security, and the environment. J. Environ. Qual. 42, 972–981.
Liu, J., Liu, H., Liu, R., Mostofa Amin, M.G., Zhai, L., Lu, H., Wang, H., Zhang, X., Zhang, Y., Zhao, Y., Ding, X., 2018. Water quality in irrigated paddy systems. In: Gabrijel, O. (Ed.), Irrigation in Agroecosystems. IntechOpen, Rijeka (Ch. 7 pp.).
Liu, Y., Tang, R., Li, L., Zheng, G., Wang, J., Wang, G., Bao, Z., Yin, Z., Li, G., Yuan, J., 2023. A global meta-analysis of greenhouse gas emissions and carbon and nitrogen losses during livestock manure composting: influencing factors and mitigation strategies. Sci. Total Environ. 885, 163900.
Ma, R., Yu, K., Xiao, S., Liu, S., Ciais, P., Zou, J., 2022. Data-driven estimates of fertilizer-induced soil NH_3, NO and N_2O emissions from croplands in China and their climate change impacts. Glob. Chang. Biol. 28, 1008–1022.
New, M., Lister, D., Hulme, M., Makin, I., 2002. A high-resolution data set of surface climate over global land areas. Clim. Res. 21, 1.
Poggio, L., de Sousa, L.M., Batjes, N.H., Heuvelink, G.B.M., Kempen, B., Ribeiro, E., Rossiter, D., 2021. SoilGrids 2.0: producing soil information for the globe with quantified spatial uncertainty. SOIL 7, 217–240.
Posch, M., Reinds, G.J., 2009. A very simple dynamic soil acidification model for scenario analyses and target load calculations. Environ. Model Softw. 24, 329–340.
Reinds, G.J., de Vries, W., 2010. Uncertainties in critical loads and target loads of sulphur and nitrogen for European forests: analysis and quantification. Sci. Total Environ. 408, 1960–1970.
Reinds, G.J., Van Oijen, M., Heuvelink, G.B.M., Kros, H., 2008. Bayesian calibration of the VSD soil acidification model using European forest monitoring data. Geoderma 146, 475–488.
Reuss, J.O., Cosby, B.J., Wright, R.F., 1987. Chemical processes governing soil and water acidification. Nature 329, 27–32.
Rowell, D.L., Wild, A., 1985. Causes of soil acidification: a summary. Soil Use Manag. 1, 32–33.
Sahrawat, K.L., 1982. Nitrification in some tropical soils. Plant Soil 65, 281–286.
Shuman, L.M., Boswell, F.C., Ohki, K., Parker, M.B., Wilson, D.O., 1983. Effects of HC1 acid and lime amendments on soil pH and extractable Ca and Mg in a sandy soil. Commun. Soil Sci. Plant Anal. 14, 481–495.
Slessarev, E.W., Lin, Y., Bingham, N.L., Johnson, J.E., Dai, Y., Schimel, J.P., Chadwick, O. A., 2016. Water balance creates a threshold in soil pH at the global scale. Nature 540, 567–569.
Song, Y., Wang, Y., Mao, W., Sui, H., Yong, L., Yang, D., Jiang, D., Zhang, L., Gong, Y., 2017. Dietary cadmium exposure assessment among the Chinese population. PLoS One 12, e0177978.
Sumner, M.E., 1994. Measurement of soil pH: problems and solutions. Commun. Soil Sci. Plant Anal. 25, 859–879.
Tang, C., Rengel, Z., 2003. Role of plant cation/anion uptake ratio in soil acidification. In: Rengel, Z. (Ed.), Handbook of Soil Acidity. Marcel Dekker, pp. 57–81.
Van Breemen, N., Driscoll, C.T., Mulder, J., 1984. Acidic deposition and internal proton sources in acidification of soils and waters. Nature 307, 599–604.
Wall, D.H., Six, J., 2015. Give soils their due. Science 347, 695.
Wang, C., Cheng, K., Ren, C., Liu, H., Sun, J., Reis, S., Yin, S., Xu, J., Gu, B., 2021. An empirical model to estimate ammonia emission from cropland fertilization in China. Environ. Pollut. 288, 117982.
Xu, D., Zhu, Q., Ros, G., Cai, Z., Wen, S., Xu, M., Zhang, F., de Vries, W., 2022. Calculation of spatially explicit amounts and intervals of agricultural lime applications at county-level in China. Sci. Total Environ. 806, 150955.
Xu, D., Zhu, Q., Ros, G.H., Xu, M., Wen, S., Zhang, F., de Vries, W., 2023. Model-based optimal management strategies to mitigate soil acidification and minimize nutrient losses for croplands. Field Crop Res. 292, 108827.
Xue, N., Seip, H.M., Liao, B., Vogt, R.D., 2003. Studies of acid deposition and its effects in two small catchments in Hunan, China. Hydrol. Earth Syst. Sci. 7 (3), 399–410 (-0001-11-30) 7.
Yu, T.R., 1988. Soil acidity characteristics and acidification problems in China. Chin. J. Soil Sci. 20, 49–51.
Zeng, M., de Vries, W., Bonten, L.T., Zhu, Q., Hao, T., Liu, X., Shen, J., 2017. Model-based analysis of the long-term effects of fertilization management on cropland soil acidification. Environ. Sci. Technol. 51, 3843–3851.
Zhao, Y., Wang, M., Hu, S., Zhang, X., Ouyang, Z., Zhang, G., Shi, X., 2018. Economics-and policy-driven organic carbon input enhancement dominates soil organic carbon accumulation in Chinese croplands. Proc. Natl. Acad. Sci. 115, 4045–4050.
Zhou, H., 2015. Effects of Cropland Soil Acidification and Remediation in Jiaodong of Shandong Province. Ph.D. Dissertation. China Agricultural University, Beijing, China.
Zhou, X., 2017. Soil Acidification in Southern China: Spatio-temporal Evolution and Effects on Phosphorus Availability. Université de Liège, Liège, Belgique (Dissertation for the Doctoral Degree).
Zhu, H., Chen, C., Xu, C., Zhu, Q., Huang, D., 2016. Effects of soil acidification and liming on the phytoavailability of cadmium in paddy soils of central subtropical China. Environ. Pollut. 219, 99–106.
Zhu, Q., de Vries, W., Liu, X., Hao, T., Zeng, M., Shen, J., Zhang, F., 2018a. Enhanced acidification in Chinese croplands as derived from element budgets in the period 1980–2010. Sci. Total Environ. 618, 1497–1505.
Zhu, Q., Liu, X., Hao, T., Zeng, M., Shen, J., Zhang, F., de Vries, W., 2018b. Modeling soil acidification in typical Chinese cropping systems. Sci. Total Environ. 613–614, 1339–1348.
Zhu, Q., Liu, X., Hao, T., Zeng, M., Shen, J., Zhang, F., de Vries, W., 2020. Cropland acidification increases risk of yield losses and food insecurity in China. Environ. Pollut. 256, 113145.
Zuo, W., Yi, S., Gu, B., Zhou, Y., Qin, T., Li, Y., Bai, Y., 2023. Crop residue return and nitrogen fertilizer reduction alleviate soil acidification in China's croplands. Land Degrad. Dev. 34, 3144–3155.